On the relation of the ripple artifact in Multi-Spectral Imaging and susceptibility induced field gradients

Chiel J den Harder[1], Ulrike A Blume[2], Gert van IJperen[1], and Clemens Bos[3]

[1]MRI Technology Development, Philips, Best, Noord Brabant, Netherlands, [2]Imaging Systems, Philips, Hamburg, Hamburg, Germany, [3]Image Sciences Institute, University Medical Center Utrecht, Utrecht, Utrecht, Netherlands

Introduction

Multi-Spectral Imaging (MSI) techniques [1,2] have been shown to significantly reduce susceptibility artifacts. Residual intensity fluctuations, referred to as pile-up artifact [3], spider-web artifact [4], or ripple artifact [1], exist as a result of limitations of the frequency encoding process and discontinuities between slices [5]. Especially in techniques that use gradient selection, such as Slice Encoding for Metal Artifact Correction (SEMAC) [1], ripple artifacts can be prominent. In this work, an analysis is presented of the effect of local field gradients in SEMAC, and of the conditions that cause the ripple artifact to become visible.

Theory

Ideally, SEMAC would completely resolve in-plane distortions by using View Angle Tilting (VAT, [6]), and slice distortions by through-plane phase encoding. However, susceptibility induced field gradients will compromise the frequency encoding process as explained in fig.1. Slice selections traverse the image sections in regions where B0 varies in-plane (fig.1a). Still, selected regions remain spectrally and spatially contiguous, which would lead to homogeneous image results, even if B0 varies through-plane (fig.1b), and slice profiles are stretched or compressed in slice direction. By frequency encoding with VAT, magnetization from a physical position (m, s) is mapped to an imaged position (m',s) where m' is given by:

$$m' = m + \frac{\Delta B0(m,s) + (s - s_{ISC})\, G_{VAT}}{G_M},$$

with G_{VAT} being the VAT gradient, G_M the read-out gradient, $\Delta B0(m,s)$ the main field deviation, and s_{ics} the intended position for the slice center. Now, if B0 only varies through-plane (center regions in fig.1c,d), all slices remain parallel to the imaging sections, leaving no intensity fluctuations in the image. However, where B0 varies in read-out direction (dB0/dm ≠ 0), frequency encoding limitations lead to compression and dilation of imaged slice profiles in the m',s-frame (fig.1c). In this frame, gaps appear where no signal ever is mapped to. If dB0/ds = 0, a slice may distort out of a section, e.g. at m_1, yet the adjacent slice will simultaneously distort into the same section (fig.1c), such that a nearly constant signal is obtained, originating from a single or two adjacent slice excitations. It is only when B0 varies both in-plane and through-plane (fig.1d) that these gaps will be wide enough to be resolved, e.g. at m'_1, allowing substantial intensity variations to arise. Localization in in-plane phase direction is by phase encoding only, which is spatially accurate, and will not be considered in the rest of this work. Finally, although SEMAC originally was presented using approximately rectangular slice profiles, Gaussian slice profiles can be used as well, as long as they match the condition $\sum_n F(\omega_n)^2 \propto 1$ for homogeneous image combination, where $F(\omega_n)$ is the spectral response of slice selection.

Methods

Simulations: Time domain MRI simulations were run to estimate the B0 variation required for the ripple artifact to become visible, and to include effects of the finite reconstruction grid in slice direction. A two-dimensional digital phantom was used with B0 varying linearly both in frequency encoding and slice direction: the B0 field had three regions with dB0/dm = -6 mT/m, dB0/dm = 0 and dB0/dm = 6 mT/m, respectively. Simulations were repeated for through-plane gradient strengths dB0/ds ranging from -4 mT/m to 4 mT/m. A selection gradient G_S =10mT/m was applied for excitation and refocusing of 5 slices centered at 4-mm intervals, each with a Gaussian selection profile with FWHM 5.5 mm, making the slices overlap close to $1/\sqrt{2}$ of the maximum intensity. SEMAC imaging was simulated on a 0.1 mm grid, with 15 phase encodings in slice direction and 4-mm section thickness. For dB0/ds = 0, a thinner section thickness of 2 mm was simulated as well. In-plane, the simulation had a FOV of 128 mm, 1 mm resolution and G_M = 10 mT/m. After Fourier transform, images were combined using sum-of-squares.

Phantom experiments: A stainless steel rod was positioned vertically in water. SEMAC was implemented on a 1.5T clinical scanner, and 4 mm slices with in-plane resolution of 1×1 mm were acquired in the coronal plane orthogonal to the rod and under 45° angulation. In the coronal plane, only in-plane field gradients are present, due to symmetry. By angulating the slice, through-plane field gradients are created, as well.

Results

In all simulated imaged slice selections, compression or dilation was observed where the sign of dB0/dm was opposite or equal to the frequency encoding gradient, respectively (not shown). The simulation results showed no ripple artifact when dB0/ds and G_S had equal sign (fig.2a), or without through-plane B0 variations (fig.2b). The ripple artifact was apparent only with selections and slice intervals significantly thicker than the sections due to through-plane B0 variations, starting at roughly -2 mT/m in these simulations (fig.2d). Acquiring sections substantially thinner than the slice excitation also showed the ripple artifact (fig.3b). In the phantom experiments, the ripple artifact was absent in the coronal acquisition and only appeared in the angulated acquisition with both in-plane and through-plane field variations (fig.4).

Discussion and Conclusion

The ripple artifact is an important limitation of the capability of MSI techniques to reduce metal artifacts [1,4]. Techniques exist to reduce the ripple artifact to some extent, e.g. by means of an additional B0 map generated by a separate MAVRIC acquisition [3]. The presented simulations help define the origin of the ripple artifact and provide a means to investigate ways to address it.
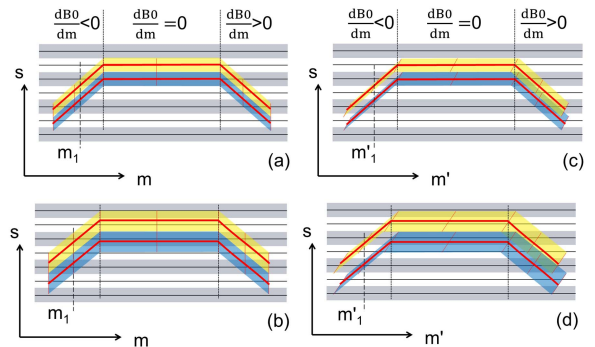

Figure 1: Adjacent slice selections (yellow/blue) for the case that B0 varies only in read-out, m (a), or both in read-out and slice, s direction (b). Readout using the VAT technique transforms the slices into their imaged equivalents (c,d) in the m', s frame. Thick red lines indicate slice selection centers, thin red lines indicate positions of constant m. Sections are indicated by grey and white bars with black centerlines.
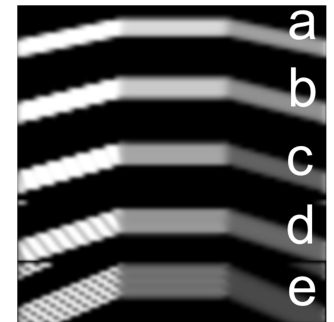

Figure 2: Simulations of SOS of 5 slice selections at 4-mm intervals. dB0/dm = -6 mT/m (left), 0 mT/m (center), +6 mT/m (right). dB0/ds = +2mT/m (a), 0 mT/m (b), -1 mT/m (c), -2 mT/m (d) and -4 mT/m (e).

Figure 3: Simulation of SOS of 5 slice selections of 4 mm thickness with dB0/ds = 0. Acquired sections of 4 mm (a) and 2 mm (b).
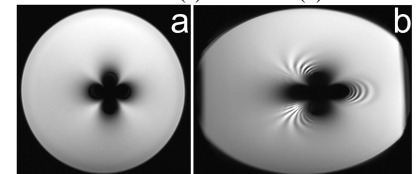

Figure 4: Stainless steel rod scanned orthogonally (a) and under 45° (b).

[1]W.Lu et al., MRM;62:66 (2009)

[2]K.Koch et al., MRM;65:71 (2011)

[3]K.Koch et al., ISMRM2011, p3173

[4]K.Koch et al., ISMRM2012, p2435

[5]B.Hargreaves et al., ISMRM2009, p258

[6]Z.H. Cho et al., Med Phys, 15:7 (1988)